Towards Globally Stable Path-Following Control of Automated Vehicles

Illés Vörös*†, Dénes Takács** and Gábor Orosz†‡
*Department of Applied Mechanics,
*Budapest University of Technology and Economics, H-1111, Hungary
⋆HUN-REN–BME Dynamics of Machines Research Group, Budapest, Hungary
†Department of Mechanical Engineering,
University of Michigan, Ann Arbor, MI 48109, USA
‡Department of Civil and Environmental Engineering,
University of Michigan, Ann Arbor, MI 48109, USA

Summary. The path-following control of automated vehicles is analyzed in the presence of large disturbances. The global dynamics of three controller variations are analyzed using phase portraits, illustrating the domain of attraction of stable path-following, the presence of possible steady state solutions and the transient response of the system. A globally stable control law is proposed, which removes all unwanted steady state solutions, guaranteeing stable path-following regardless of initial conditions and disturbances.

Introduction

This paper focuses on the global dynamics of the path-following control of automated vehicles in order to guarantee that the vehicle can safely handle unexpected, large disturbances without stability loss. Although the path-following control of vehicles is an active research field with a rich history, the nonlinear analysis of these steering controllers with the consideration of larger perturbations is less common in the literature [1].

Vehicle Model and Control Design

We use a kinematic bicycle model for our analysis, where the elasticity of the tires is neglected (see Fig. 1). The state variables of the model include the positional coordinates x_{R} and y_{R} of the rear axle center point R and yaw angle ψ. The wheelbase is denoted by l and V is the longitudinal speed of the vehicle, which is assumed to be constant. The governing equations of the system are the following:

$$\dot{x}_{\mathrm{R}} = V\cos\psi\,, \quad \dot{y}_{\mathrm{R}} = V\sin\psi\,, \quad \dot{\psi} = \frac{V}{l}\tan\delta_{\mathrm{s}}\,, \tag{1}$$

where δ_{s} is the steering angle. In order to simplify our calculations, we use $u = \tan\delta_{\mathrm{s}}$ as the control input.
The control goal is to stabilize the straight-line motion of the vehicle along the x-axis of the global reference frame. Three different controller variations are considered to achieve this. The first controller generates the control input as the linear combination of the lateral deviation and the angle error:

$$u = -P_y y_{\mathrm{R}} - P_\psi \psi. \tag{2}$$

A modified version of this controller uses the sine of the angle error, which can be shown to be equivalent to the so-called look-ahead controller:

$$u = -P_y y_{\mathrm{R}} - P_\psi \sin\psi. \tag{3}$$

The third controller is the nonlinear control law derived from the one in [2]:

$$u = -P_\psi\left(\psi + \arctan\left(\frac{P_y}{P_\psi}y_{\mathrm{R}}\right)\right), \tag{4}$$

where the arc tangent function limits the effects of large lateral errors. Note that when linearized around $y_{\mathrm{R}} = 0$ and $\psi = 0$, the control laws (3) and (4) both reduce to (2).

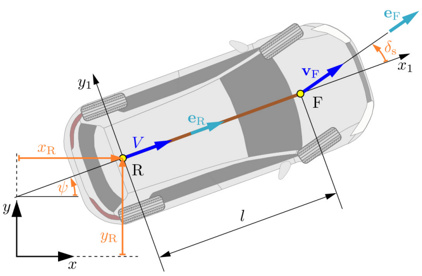

Figure 1: Kinematic vehicle model with relevant quantities marked.

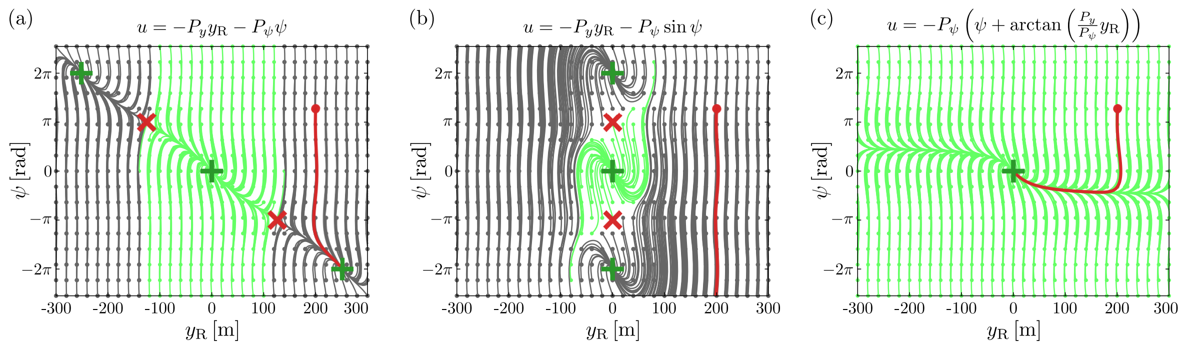

Figure 2: Phase portraits using the three control law variations.

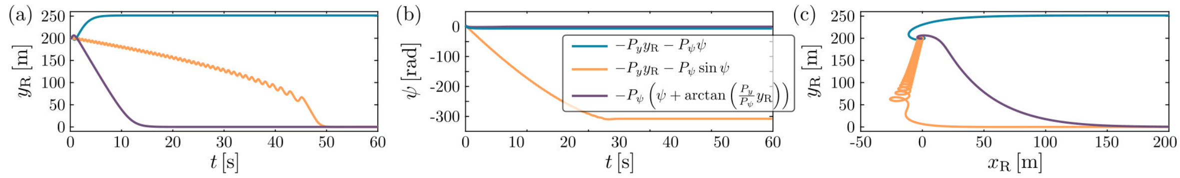

Figure 3: Lateral position (a), yaw angle (b) and the vehicle's path in the x-y plane (c) for the trajectories highlighted in red in Fig. 2.

Analysis

Figure 2 shows phase portraits of the controlled vehicle in the plane of the lateral position and yaw angle using the three different controllers defined above. The control gains are selected such that the linear behavior of the system is the same in all three cases, therefore the differences in the global dynamics can be highlighted. The possible steady states of the system are denoted by green plus signs (stable) and red crosses (unstable) in Fig. 2. The origin corresponds to the desired steady state of straight-line motion along the x-axis with zero angle error. A series of numerical simulations from a uniform grid of initial conditions have been run to illustrate the possible trajectories in the state space. Trajectories that converge to the origin are plotted in green, while the black trajectories converge to different steady states.

In case of the linear control law (Fig. 2(a)), the possible steady states of the system are $\psi^* = k\pi$ and $y_\mathrm{R}^* = -\frac{P_\psi}{P_y} k\pi$ ($k \in \mathbb{Z}$), i.e., the vehicle runs parallel to the x-axis in steady state, with some possible lateral error, which depends on the control gains. The sine function in the second control law (Fig. 2(b)) ensures that only steady states with zero lateral error are possible. Furthermore, the stable equilibrium points correspond to $\psi^* = 2k\pi$, i.e., the vehicle moves in the positive x-direction in steady state, as intended. However, the transient trajectories until the vehicle reaches the steady state can still be very undesirable. The third control law can be interpreted as generating a reference yaw angle of $\psi_\mathrm{des} = -\arctan\left(\frac{P_y}{P_\psi} y_\mathrm{R}\right)$. The arctan function limits the value of this reference angle for large lateral errors, therefore if the vehicle is far from the reference path ($y_\mathrm{R} \to \pm\infty$), the controller steers it directly toward the path ($\psi_\mathrm{des} \to \mp\pi/2$). As a result, the third control law removes all unwanted steady state solutions besides the origin, achieving global stability of the trivial equilibrium (Fig. 2(c)).

The example trajectories in Fig. 3 (that are highlighted in red in Fig. 2) show the behavior of the three control laws in case of initial conditions that far from the origin. Although control errors of this magnitude have little practical relevance, they highlight better the differences in the global dynamics of the three controllers. In case of large lateral errors, the first controller steers the vehicle to a different steady state parallel to the x-axis. The second control law eventually reaches the desired steady state, but its transient trajectory is very undesirable and unsafe in practice. The third control law is able to steer the vehicle to the desired reference path in an effective manner.

Conclusion and Discussion

A control law is developed which can ensure the global stability of the trivial equilibrium. Further development of this controller may be possible such that a given part of the state space is forward invariant which is related to the safety of automated vehicles.

Acknowledgment The research reported in this paper was partly supported by the János Bolyai Research Scholarship of the Hungarian Academy of Sciences, the National Research, Development and Innovation Office under grant no. NKFI-146201 and 2020-1.2.4-TET-IPARI-2021-00012 and by the Rosztoczy Foundation.

References

[1] Vörös, I., Orosz, G., Takács, D. (2023) On the global dynamics of path-following control of automated passenger vehicles. Nonlinear Dynamics **111**(9):8235–8252

[2] Qin, W.B., Zhang, Y., Takács, D., Stépán., G., Orosz, G. (2022) Nonholonomic dynamics and control of road vehicles: moving toward automation. Nonlinear Dynamics **110**(3):1959–2004